International Journal of Nanomedicine

Dovepress
open access to scientific and medical research

Open Access Full Text Article

ORIGINAL RESEARCH

Encapsulation of *Piper cabralanum* (Piperaceae) nonpolar extract in poly(methyl methacrylate) by miniemulsion and evaluation of increase in the effectiveness of antileukemic activity in K562 cells

Anderson Nogueira Mendes[1]
Lívia Alves Filgueiras[1]
Monica Regina Pimentel Siqueira[2,3]
Gleyce Moreno Barbosa[2]
Carla Holandino[2]
Davyson de Lima Moreira[3]
José Carlos Pinto[4]
Marcio Nele[5]

[1]Department of Biophysics and Physiology, Federal University of Piauí, Teresina, Piauí, [2]School of Pharmacy, Federal University of Rio Janeiro, [3]Natural Products Department, Institute of Pharmaceutical Technology, Farmanguinhos, Oswaldo Cruz Foundation, Rio de Janeiro, [4]Chemical Engineering Program – COPPE, Federal University of Rio de Janeiro, Rio de Janeiro [5]School of Chemistry, Federal University of Rio Janeiro, Rio de Janeiro, Brazil

Abstract: This study aimed to synthesize and characterize nanoparticles (NPs) of poly(methyl methacrylate) (PMMA) and evaluate their ability to incorporate plant extracts with antitumor activity and low dissolution in aqueous media. The extract used was *n*-hexane partition of the methanol extract of *Piper cabralanum* (PCA-HEX). PMMA NPs were obtained using the miniemulsion method, which was able to encapsulate almost 100% of PCA-HEX. The synthesized polymeric particles presented with a size of 200 nm and a negative charge. Cytotoxicity tests by MTT and trypan blue assays showed that NPs without PCA-HEX did not kill leukemic cells (K562 cells). NPs containing PCA-HEX were able to enhance cell death when compared to pure extract. The results showed that PMMA NPs could be useful as a drug delivery system as they can enhance the antitumor activity of the PCA-HEX extract by more than 20-fold. PMMA NPs containing plant extracts with antitumor activities may be an alternative to control the evolution of diseases such as leukemia.

Keywords: *Piper*, Piperaceae, nanoparticles, miniemulsion, PMMA, K562 cells, leukemia

Introduction

One of the objectives of nanotechnology is the development of products to improve the lives and health of humans. Considering the success of nanoparticles (NPs) in inhibiting tumors, the synthesis of polymeric particles has received large investments in the pharmaceutical industry.[1–4] Polymeric NPs have been considered promising for the development of drug delivery systems for oral, intramuscular, and subcutaneous use.[1,2]

The development of techniques for nanoencapsulation of drugs is necessary to improve some factors that increase the sensitivity to the bioactive compound while decreasing their systemic concentration in the body to prevent the accumulation and side effects. This technology can result in improved prognosis, especially in complex diseases such as cancer, HIV, and degenerative diseases.[2,5–8]

Different types of NPs have been investigated and used as drug carriers. NPs of poly(methyl methacrylate) (PMMA), for example, have been investigated as drug carriers against diseases such as Duchenne muscular dystrophy and cancer.[5–9] Thus, prototypes can be developed with the aim of overcoming biological barriers such as cell membranes, blood vessels, interstitial pressure gradients, and blood–brain barrier.[10]

Correspondence: Anderson Nogueira Mendes
Department of Biophysics and Physiology, Federal University of Piauí, Avenida Universitária, lado ímpar, Bairro Ininga CEP 64.049-550, Teresina, Piauí, PI, Brazil
Tel +55 86 3237 2105
Email anderson.mendes@gmail.com

submit your manuscript | www.dovepress.com
Dovepress
http://dx.doi.org/10.2147/IJN.S134756

The PMMA was first used in hip replacements in orthopedic surgery.[11] However, studies showed that PMMA may have other applications such as in bioplasty[12] and as a carrier for antitumor drugs.[9,13] PMMA NPs are biocompatible and can be produced by miniemulsion, emulsion, and suspension processes.[13,14] For example, PMMA NPs complexed with survivin may act in reducing the proliferation of human A549 cells.[9]

Cancer is a leading cause of death worldwide and a major challenge for modern chemotherapy.[4] According to GLOBOCAN 2012, it is expected that 19.3 million new cancer cases will be diagnosed every year by 2025. Surgery, radiation, chemotherapy, and immunotherapy are the primary methods for cancer therapy.[3] The construction of new efficient strategies to combat this malignancy is urgently needed to combat their high statistics of mortality and morbidity.[15]

Chronic myeloid leukemia is a malignant disorder of hematopoietic stem cells and exhibits a very aggressive clinical course.[16] It represents about 15% of all leukemias diagnosed in adults (40–60 years of age) with an incidence of 1.5/100,000 population.[17] The most common symptom of leukemia is pancytopenia or infiltration of leukemic cells.[18] The clinical manifestations appear as a result of the excessive proliferation of immature cells when the disease has been practically installed.[18,19] Being a myeloproliferative disease, it is associated with an increase in white blood cells, splenomegaly, weight loss, anemia, and lethargy.[19] Therefore, prompt treatment aimed at the destruction of these tumor cells, thus enabling the bone marrow to produce normal cells, should be given.[18]

Plant extracts have been used in the treatment of breast cancer, AIDS, and tuberculosis.[20] In Brazil, the species *Piper cabralanum* has aroused great interest, because it has substances that are active against several diseases. This species is endemic in the Atlantic Forest.[21] Piperaceae extracts have shown antileukemic activity.[21–25] The presence of substitute phenolic groups for compounds, such as chalcones, has motivated the study of Piperaceae extracts against cancer. The chalcones are described as promising drugs for antitumor treatment, which they demonstrate by inducing three different effects: antioxidants, cytotoxic, and apoptosis-inducing.[22]

Considering these aspects, the present study aimed to evaluate the efficiency of the encapsulation of *P. cabralanum* nonpolar extract in PMMA NPs. PMMA NPs containing *n*-hexane extract of this plant in miniemulsion method was performed. Subsequently, NPs were assayed in vitro against K562 tumor cell line in order to check whether PMMA NPs increase the activity of the *n*-hexane extract of *P. cabralanum*.

Materials and methods

Materials

Methyl methacrylate, sodium dodecyl sulfate, sodium persulfate, hexadecane, and sodium bicarbonate were purchased from Sigma-Aldrich Co (St Louis, MO, USA). The *n*-hexane extract of *P. cabralanum* C.DC. (Piperaceae), named as PCA-HEX, was prepared as described earlier.[21] Briefly, plant material was collected in Teresópolis/RJ, Brazil (GPS location 22°24′48″S 42°59′24″W). The leaves were extracted with methanol (HPLC grade), and the methanol extract was partitioned with *n*-hexane, dichloromethane, ethyl acetate, and *n*-butanol.[21] The nonpolar *n*-hexane extract was used in this study. Rhamnolipids were produced as described by Mendes et al.[26]

Synthesis of PMMA NPs containing PCA-HEX

NPs were prepared by a miniemulsion process oil-in-water. The PCA-HEX was solubilized in a mixture containing 1.8 g of hexadecane and 58.2 g of methyl methacrylate under constant stirring for 5 minutes at 150 rpm. The production processes of PMMA NPs containing PCA-HEX extract were standardized to 58.8 mg/g (PCA-HEX/MMA). The hydrophobic solution was added to 240 g of an aqueous solution containing 0.4 g of sodium bicarbonate, 1 g/L of rhamnolipid, or 10 g/L of sodium dodecyl sulfate and stirred for 3 minutes at 150 rpm. Then, the samples were sonicated using a Sonics ultrasound system (VCX750; Sonics & Materials Inc., Newton, CT, USA) for 4 minutes at 40% amplitude. Finally, the miniemulsion thus obtained was transferred to a controlled reactor EasyMax 102 (Mettler Toledo, Columbus, OH, USA).

The polymerization process was started with the addition of sodium persulfate (0.33%/g). The miniemulsion was maintained at controlled temperature (80°C for 3 hours at 250 rpm). During the polymerization process, samples were collected to investigate the polymerization mechanism. Gravimetric analyses were used to confirm the polymerization process.

Three types of PMMA polymeric NPs were produced: PMMA NPs containing PCA-HEX where rhamnolipid was used as a surfactant (PMMA-RML-PCA-HEX); PMMA NPs without PCA-HEX and rhamnolipid as surfactant (PMMA-RML); PMMA NPs without PCA-HEX and sodium dodecyl sulfate as surfactant (PMMA-SDS).

Fourier-transform infrared spectroscopy

The samples of NPs were mixed with potassium bromide (KBr) at a ratio of 1% (w/w) and characterized by Fourier-transform

infrared spectroscopy (FT-IR) using infrared spectrophotometer model 6700 (FT-IR Nicolet; Thermo Fisher Scientific, Waltham, MA, USA) where spectral scan was performed between 500 and 4,000 cm^{-1}.

Conversion by gravimetry

The conversion was gravimetrically determined based on the ratio between the mass of polymer present in the reactor and the mass of monomer fed. The polymer mass was calculated from the dried residue obtained by evaporation of a latex sample in an oven with forced ventilation.

Analysis by scanning electron microscopy

Analysis of the morphology of the polymeric NPs was performed by scanning electron microscopy (SEM) using the equipment SEM Quanta 200 from FEI Company (Hillsboro, OR, USA).

Gel permeation chromatography

Gel permeation chromatography (GPC) was used to determine the molecular weight distribution of the polymers produced. Molecular weight distribution analysis was carried out in the VE2001 Viscotek GPC system (Houston, TX, USA). The chromatographic conditions were as follows: tetrahydrofuran as mobile phase (1 mL/min), injection volume of 100 uL, detector for refractive index (EV 3580), Phenomenex columns (500 Å, 10,000 Å, 100,000 Å, 1,000,000 Å) at 40°C. Samples were prepared by weighing ~10 mg of sample in a 10 mL volumetric flask and the final concentration was made in a mixture of methanol and an aqueous solution containing 0.1 wt% of formic acid.

Differential scanning calorimetry

Analyses were performed using the technique of differential scanning calorimetry (DSC) in a Perkin-Elmer Diamond DSC equipment (PerkinElmer, Inc, Waltham, MA, USA). About 3 mg of each sample was weighed and subjected to heating from 25°C to 200°C at a heating rate of 10°C/min. Tg (glass transition temperature) was performed during the second heating ramp to eliminate the thermal history of the polymer. Nitrogen was used as a carrier gas at a flow rate of 80 mL/min.

Zeta potential

The zeta potential and dynamic light scattering particle size of the NPs was measured using a zeta potential meter (Zetasizer Nano ZS) at 37°C. An analyzer (INNDVO300/BI900AT; Brookhaven Instruments, Holtsville, NY, USA) was used to determine the hydrodynamic radii and polydispersity of NPs at 37°C.

Cytotoxic activity of polymeric NPs

PMMA NPs were resuspended in culture medium and subsequently filtered through a millipore membrane 0.45 µm for cytotoxic activity tests. The antitumor activity was studied on human tumor cell line K562 purchased from American Type Culture Collection (ATCC CCL-243; Rockefeller, MD, USA) having a concentration of 5×10^5 cells/mL. The concentrations applied in leukemic cells ranged from 150 µg/mL to 1,500 µg/mL for determination of the minimum inhibitory concentration. Cytotoxicity was determined using trypan blue (TB) and MTT assays, as described by Mendes et al.[13]

Hemolytic activity

The hemolytic activity was investigated by incubating a suspension of sheep red blood cells (RBCs) and NPs of PMMA as described by Sperandio et al.[27] Sheep RBCs were washed three times in PBS (pH 7.2, 0.8% NaCl, 0.02% KCl, 0.17% Na2HPO4, and 0.8% KH2PO4) and resuspended in PBS at a density of 5×10^8 cells/mL at 4°C. Hemolysis assays were performed by mixing 100 µL of RBCs and 100 µL of PMMA NPs (1,500 µg/mL) or PCA-HEX (1,500 µg/mL) in PBS and incubating at 37°C for 1 hour. After centrifugation, the release of hemoglobin was measured in 100 µL of cell supernatant at 540 nm. The absence of hemolysis (blank control) or total hemolysis (positive control) was determined by replacing with 100 µL of PBS or Milli-Q sterile water, respectively. The results were determined by the percentage of hemolysis in the sample compared to the positive control (100% hemolysis), and the experiments were performed in triplicate.

Statistical analysis

All assays were performed in triplicate and in three independent experiments. The half-maximal inhibitory concentration (IC^{50}) values and 50% cytotoxicity concentration values, with 95% confidence intervals, were calculated using a probit regression model and Student's *t*-test. Analysis of variance (ANOVA) followed by a Bonferroni test were performed, taking a *P*-value of <0.05 as the minimum level required for statistical significance.

Results and discussion

Synthesis and characterization of polymeric NPs of PMMA

The different methods used for obtaining PMMA NPs are capable of producing NPs of different sizes and molar masses.

The polymerization process may be tuned to modify the size of the polymer chains.[28]

Figure 1 shows that the polymerization rate was similar under all the conditions. The initiator sodium persulfate was added into the homogenizer during emulsion preparation. The concentration of PMMA increased with time with the proceeding of the reaction. The reactions followed a polynomial mathematical model as described in Figure 1. The polymerization rate presented small difference between PMMA-SDS, PMMA-RML, and PMMA-RML-PCA-HEX. All polymerization processes showed a short induction period before the start of the reaction. After 180 minutes of reaction, 100% of the monomer was converted to polymer. Figure 1A–C indicates that in all processes there was depletion of the monomer in the bulk.

Figure 2 shows the infrared spectra (FT-IR). The infrared spectrometry allows evaluation of the presence of chemical interactions between polymers and drugs or other molecules, thus constituting an important tool in the characterization of the formulated polymers.[29] The FT-IR spectrum (Figure 2) shows details of functional groups present in the synthesized PMMA. Signals at 2,990 and 2,950 cm^{-1} can be assigned to axial strain C–H bonds of aliphatic carbon (can be assigned to stretching vibrations of the $-CH_3$ and $-CH_2-$ groups). A sharp and intense signal at 1,724 cm^{-1} can be assigned to the axial deformation of an ester carbonyl grouping (C=O). The presence of only one signal indicates the homogeneity of the polymer (only one type of carbonyl group).

The signal around 1,430 cm^{-1} is attributable to the angular deformation of C–H bond, corroborating the aliphatic portion of the polymer. The region comprising the range 1,250–1,000 cm^{-1} showed signals relating to the angular deformation of C–O ester bonds.[30] PMMA samples present as main peaks, $O-CH_3$ (2,850–2,815 cm^{-1}); –C=O (1,650–1,790 cm^{-1}); $-CH_3$ (1,430–1,470 cm^{-1}),[31] confirming the spectra obtained. The results of FT-IR showed that the compounds of PCA-HEX did not interfere in the polymer chain.

The thermoanalytical methods such as DSC and techniques involving the determination of molecular weight distribution have been used to investigate the interactions between the polymer and the drug in different formulations of microspheres and NPs.[32–35]

Figure 3 shows the thermogravimetric analysis of polymeric NPs of PMMA. Analyses of thermogravimetry showed no variations. However, PMMA-RML (Figure 3B) and PMMA-RML-PCA-HEX (Figure 3C) varied in the presence of initial plateau decomposition. This plateau (marked with

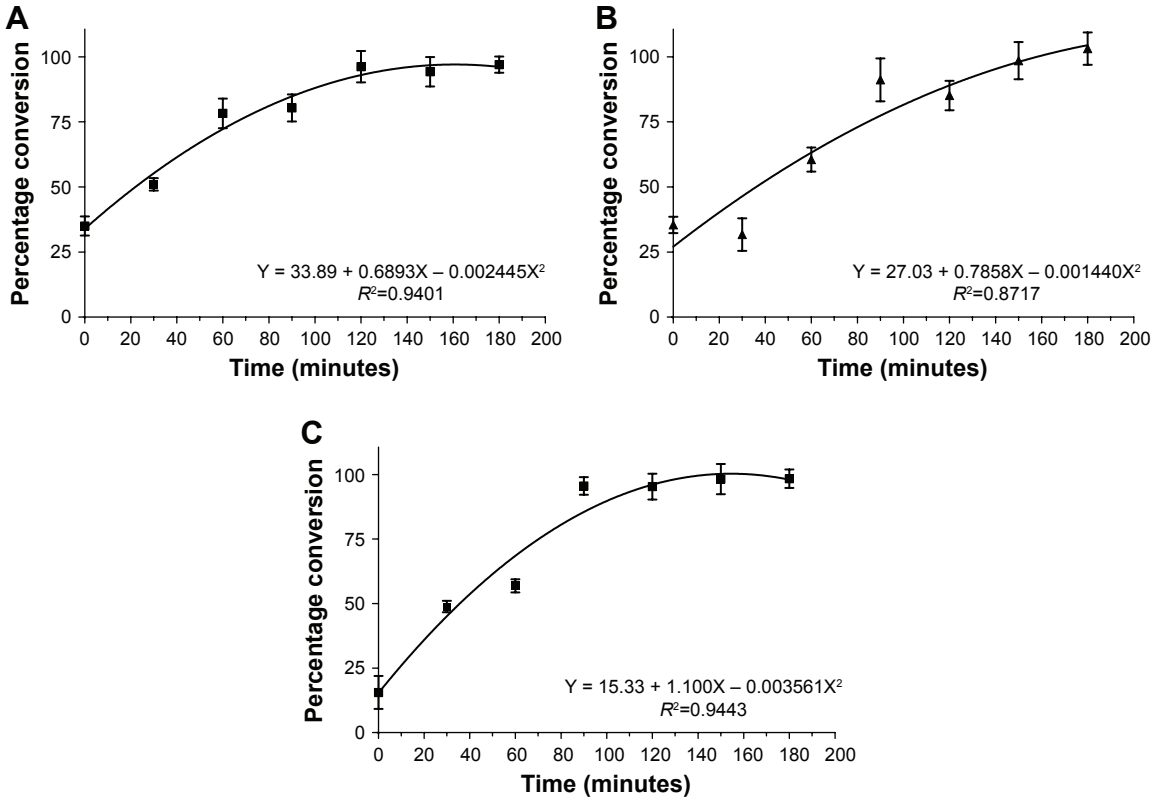

Figure 1 Evolution of the polymerization rate: (**A**) PMMA-SDS, (**B**) PMMA-RML, and (**C**) PMMA-RML-PCA-HEX.
Abbreviations: PMMA, poly(methyl methacrylate); SDS, sodium dodecyl sulfate; RML, rhamnolipid; PCA-HEX, *n*-hexane extract of *Piper cabralanum* C.DC.

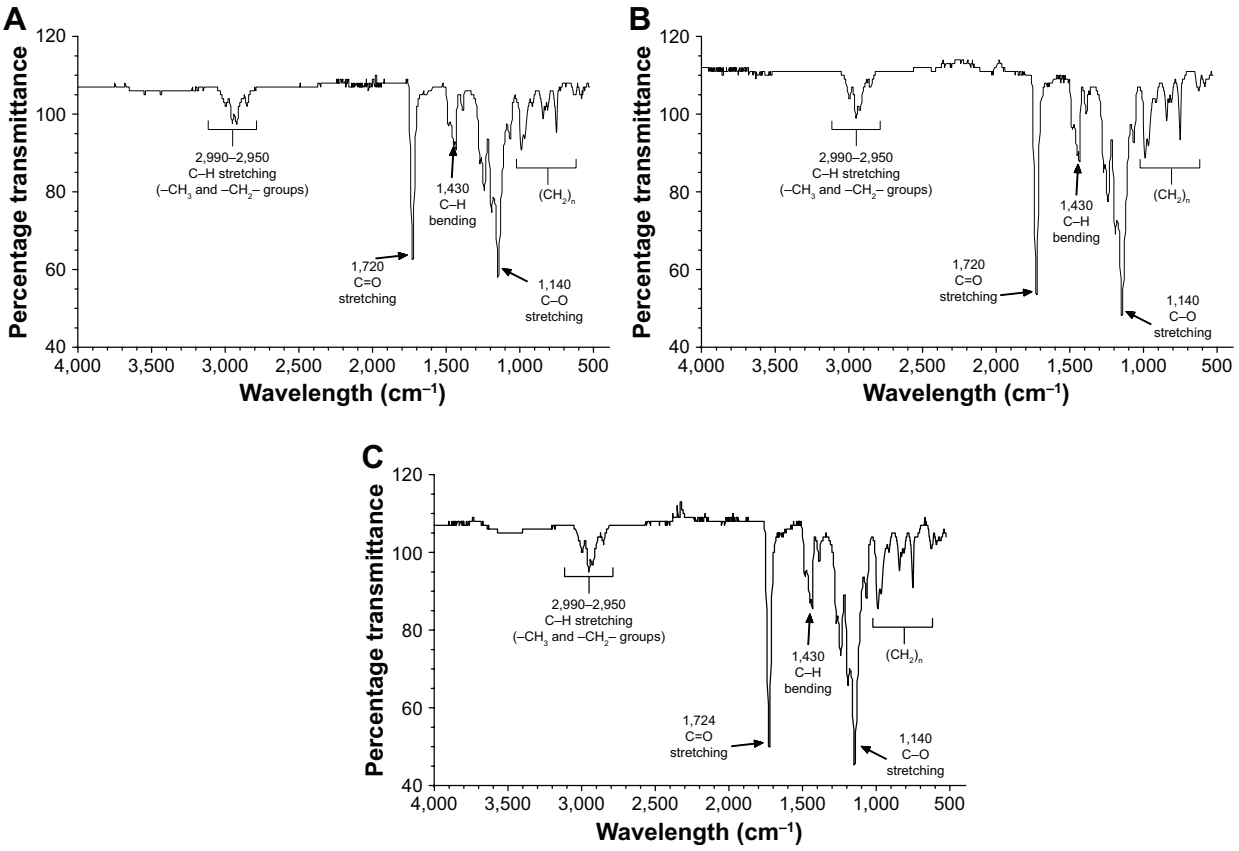

Figure 2 FT-IR spectrum of PMMA nanoparticles: (**A**) PMMA-SDS, (**B**) PMMA-RML, and (**C**) PMMA-RML-PCA-HEX.
Abbreviations: PMMA, poly(methyl methacrylate); SDS, sodium dodecyl sulfate; RML, rhamnolipid; PCA-HEX, *n*-hexane extract of *Piper cabralanum* C.DC.

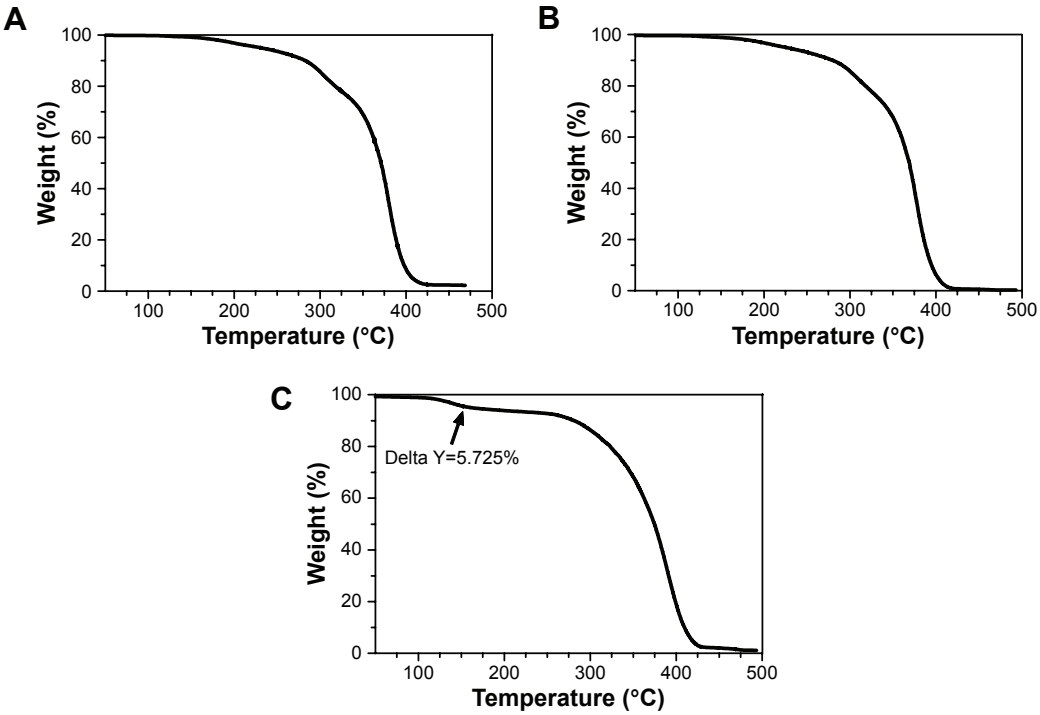

Figure 3 TGA thermogram of PMMA nanoparticles: (**A**) PMMA-SDS, (**B**) PMMA-RML, and (**C**) PMMA-RML-PCA-HEX.
Note: The arrow indicates the decomposition of PCA-HEX.
Abbreviations: TGA, thermal gravimetric analysis; PMMA, poly(methyl methacrylate); SDS, sodium dodecyl sulfate; RML, rhamnolipid; PCA-HEX, *n*-hexane extract of *Piper cabralanum* C.DC.

a black arrow) is possibly associated with the decomposition of the compounds in the PCA-HEX extract.

According to Figure 3C, the mass fraction of the extract was about 5.7%. Assuming this level was solely due to the decomposition of the extract, the PCA-HEX value relative to the total weight would be around 57.25 mg/g, which corresponds to an encapsulation efficiency of 98.7%. This percentage indicates that the nonpolar *n*-hexane extract was efficiently encapsulated.

Figure 4 shows the glass transition of the polymeric NPs. According to the analysis, rhamnolipid, SDS, and PCA-HEX did not modify the polymeric structure of PMMA. All samples have the same melting point and/or crystallization. This statement confirmed the FT-IR analysis. Figure 3 shows that the curves overlap. The DSC was important to observe the melting and crystallization of sample. Based on the thermograms obtained from the analyses of samples in the DSC, an average and standard deviation of Tg was calculated for each independent sample, to verify that the polymers produced could differ in Tg values. According to literature, the Tg of pure PMMA was found to be 105°C.[36] However, the Tg of commercial products can vary from 85°C to 165°C.[36–38] The Tg of all polymers produced were within the accepted ranges (ie, about 105°C).

Figure 5 shows the average molecular weight of the polymeric NPs obtained by GPC. The molar mass may be calculated taking into account the number average molecular weight (Mn) and weight average molar mass (Mw). The polydispersity index can be evaluated using the Mw/Mn ratio. When the polydispersity is low, it can be considered that the analyzed molecules have similar molecular weights.

The PMMA-RML-PCA-HEX has lower Mw and Mn, which indicates that the RML and the PCA-HEX may possibly have acted as chain transfer agents, reducing the molecular weight without interfering with the conversion and without being incorporated into the polymer chain, as suggested by FT-IR and DSC results. According to the data, the Mn/Mw ratio for the PMMA-SDS, PMMA-RML, and PMMA-RML-PCA-HEX was 2.6±1.5, 2.9±2.0, and 2.5±2.2, respectively.

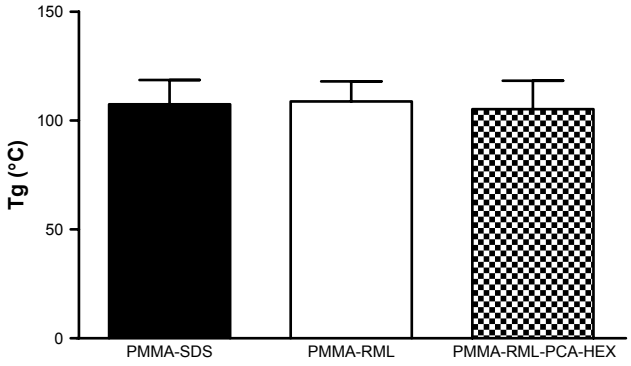

Figure 4 Glass transition temperature (Tg) of the polymers.
Abbreviations: PMMA, poly(methyl methacrylate); SDS, sodium dodecyl sulfate; RML, rhamnolipid; PCA-HEX, *n*-hexane extract of *Piper cabralanum* C.DC.

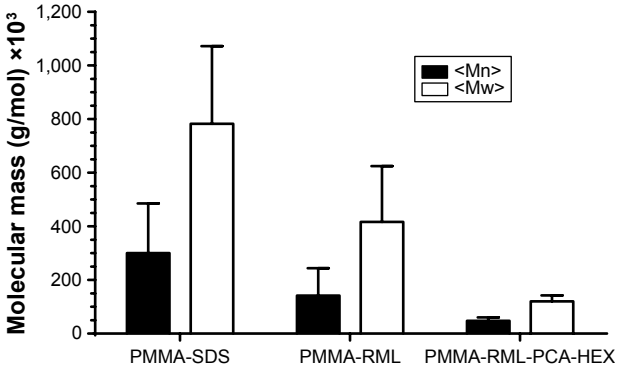

Figure 5 Average molar mass of the polymers.
Abbreviations: PMMA, poly(methyl methacrylate); SDS, sodium dodecyl sulfate; RML, rhamnolipid; PCA-HEX, *n*-hexane extract of *Piper cabralanum* C.DC.; Mn, umber average molecular weight; Mw, weight average molar mass.

The charge and size of a NP are important features that determine their physical and chemical characteristics. Figure 6 shows the analysis of particle size and zeta potential of the obtained polymeric NPs. Figure 6A–C shows PMMA-SDS NPs with size 58.9±4.4 nm, PMMA-RML with size 148.1±5.3 nm, and PMMA-RML-PCA-HEX with size 142.8±6.8 nm. The hydrodynamic size by dynamic light scattering (Figure 6D) was confirmed by the results obtained by SEM. All NPs presented with spherical morphology. Figure 6E shows the zeta potential of the NPs, which is as follows: PMMA-SDS, −42.50±2.2 mV; PMMA-RML, −55.40±5.1 mV; and PMMA-RML-PCA-HEX, −61.10±3.1 mV. PMMA-SDS has lower negative charge, while PMMA-RML and PMMA-RML-PCA-HEX have greater load.

The zeta potential can be used as an additional parameter to verify the stability of colloidal dispersions. For small molecules and particles, a high zeta potential is associated with dispersion, thus decreasing the aggregation phenomena. When the potential is low, attraction overcomes repulsion inducing aggregation, coagulation, or flocculation. So colloids with high zeta potential (negative or positive) are electrically stabilized, while colloids with low zeta potential tend to coagulate or flocculate.[39] The zeta potential results of the NPs were obtained in solutions with pH 7.4 (physiological pH). Thus, in the physiological media the NPs of PMMA apparently do not undergo aggregation processes. In the

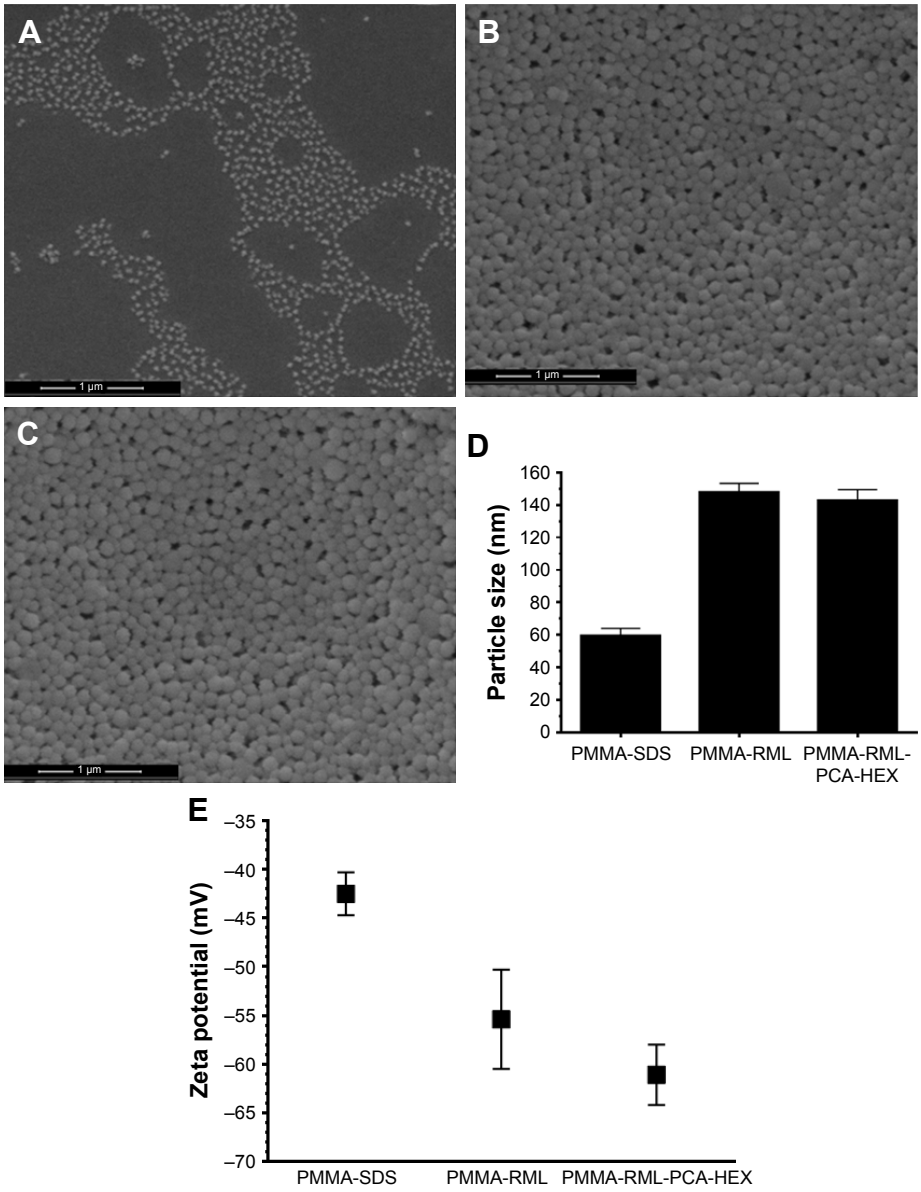

Figure 6 Morphology of the polymeric nanoparticles. (**A**–**C**): scanning electron microscope images of nanoparticles – (**A**) PMMA-SDS, (**B**) PMMA-RML, and (**C**) PMMA-RML-PCA-HEX. (**D**) Size of polymeric nanoparticles by dynamic light scattering. (**E**) Zeta potential of the polymeric nanoparticles.
Abbreviations: PMMA, poly(methyl methacrylate); SDS, sodium dodecyl sulfate; RML, rhamnolipid; PCA-HEX, *n*-hexane extract of *Piper cabralanum* C.DC.

present study, the zeta potential in different acidic and basic media was not evaluated, since the acidic and basic properties could alter the structure of the NPs and the components of PCA-HEX.

Cytotoxicity test of PMMA NPs

Cytotoxicity was measured after 1 and 24 hours based on two methods, TB (Figure 7A–D) and MTT (Figures 7E–H) assays. Figure 7A–D shows the permeability of TB into the K562 cells treated with different concentrations of NPs. PMMA-SDS and PMMA-RML NPs did not induce incorporation of TB for 1 hour and 24 hours.[13] PMMA-RML-PCA-HEX induced cell death in 1 hour (Figure 7A) and 24 hours (Figure 7C). As a positive control, K562 cells were treated with PCA-HEX (Figure 7B, D, and F). PMMA-RML-PCA-HEX showed increased cell permeability to TB, indicating that the PCA-HEX nanoencapsulation increases the cytotoxic activity of the extract, as shown in Figure 7A and C. Figure 7A shows that after 1 hour of treatment with 800 µg/mL, PMMA-RML-PCA-HEX induced permeabilization in 50% of K652 cells. The PCA-HEX induced permeabilization in 20% at the same concentration (Figure 7B). After 24 hours of treatment (Figure 7C and D), the permeability to TB reached 100% at 600 µg/mL concentration. Induction of

cell permeability is indicative of changes in cell membrane that may be occurring when cells are sensitized with the PCA-HEX. The TB influx has been used in the literature as a cell viability marker. When the cell membrane loses its integrity, large molecules become permeable, indicating a possible sign of cell death.[40–43]

To evaluate the cytotoxicity of polymeric NPs, the MTT assay was used, which evaluates mitochondrial integrity and is widely used to check the cell activity. Figure 7E and F shows the cytotoxic activity of polymeric NPs in K562 cells. The PMMA-RML and PMMA-SDS did not induce cell death (Figure 7G and H). These data corroborate with those described in the literature, since NPs containing PMMA are not cytotoxic.[13] Our results indicated that PCA-HEX and PMMA-RML-PCA-HEX induced cell death. The IC^{50} value calculated for PMMA-RML-PCA-HEX was 350 µg/mL and for PCA-HEX was 460 µg/mL. As demonstrated in the TB assay, NPs increased cytotoxic activity of the nonpolar *n*-hexane extract, which has also been demonstrated in the MTT test.

The permeabilization and cytotoxicity assays were performed after the dilution of all materials in the culture medium following lyophilization. Thus, it should be noted that PMMA NPs contained only 5% PCA-HEX. This demonstrates that the effectiveness with respect to PCA-HEX permeation and cytotoxicity has been potentiated to more than 20-fold. Assuming the proportion of 5% PCA-HEX in the NP, one can conclude that the IC^{50} of PC-HEX is 17.5 µg/mL. In parallel, cell permeability was induced with 30 µg/mL concentration in 24 hours. Both effects are indications of the effectiveness of the encapsulation process by increasing the potency of the extract. PMMA NPs do not induce cytotoxicity and permeability. In this study, the

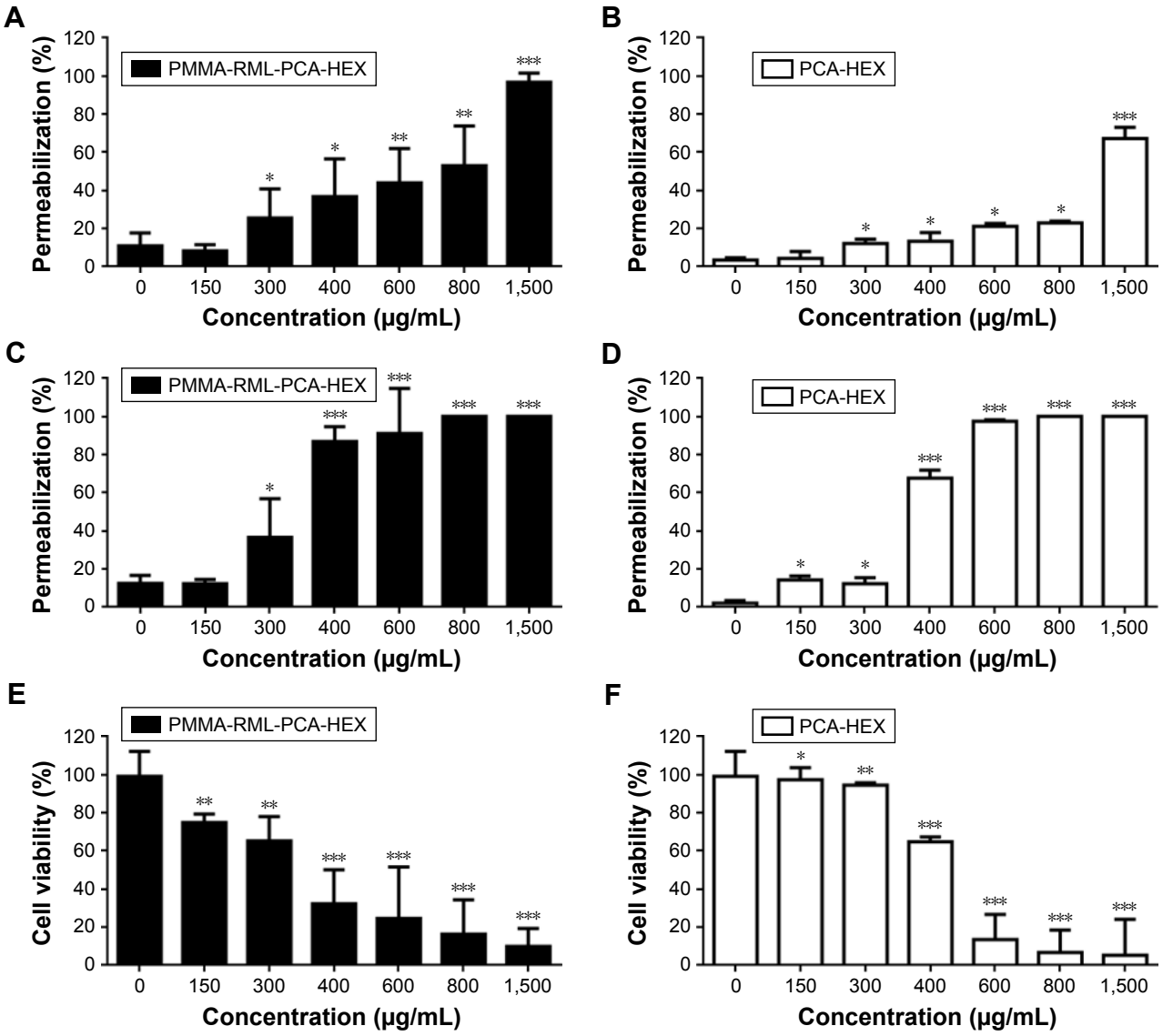

Figure 7 (*Continued*)

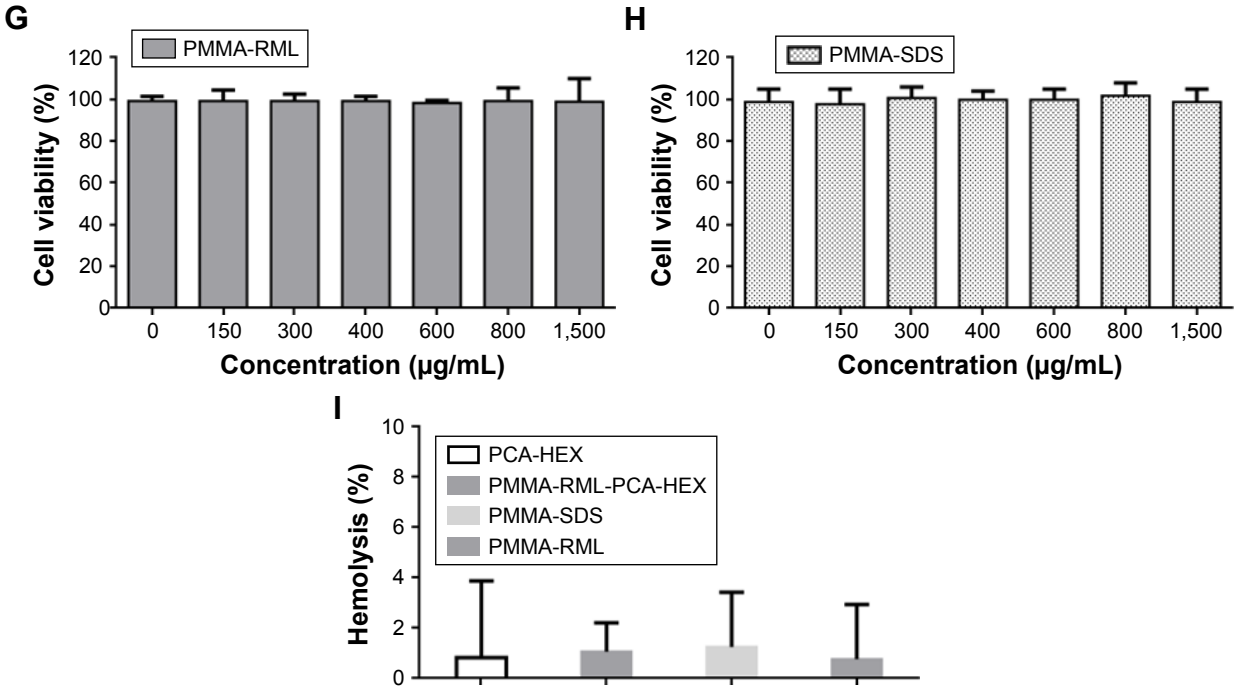

Figure 7 Cytotoxic activity of nanoparticles in human leukemic cell line K562 and hemolytic activity.
Notes: (**A**–**D**): the effect of polymeric nanoparticles on permeation rate measured by trypan blue exclusion. Permeabilization effect after 1 hour of exposure to (**A**) PMMA-RML-PCA-HEX and (**B**) PCA-HEX. Permeabilization effect after 24 hours of exposure to (**C**) PMMA-RML-PCA-HEX and (**D**) PCA-HEX. (**E**–**H**): cytotoxic effect of polymeric nanoparticles on the viability of human K562 cells. Cytotoxicity effect after 24 hours of exposure to (**E**) PMMA-RML-PCA-HEX and (**F**) PCA-HEX. Cytotoxicity effect after 24 hours of exposure to (**G**) PMMA-RML and (**H**) PMMA-SDS. Viability was determined using MTT assay, and the optical density was determined at 540 nm. (**I**): hemolytic activity of nanoparticles in a 5% suspension of human O^- red blood cells after 1 hour of incubation. Data represent the mean of three experiments in triplicate. *$P<0.05$; **$P<0.01$; ***$P<0.001$.
Abbreviations: PMMA, poly(methyl methacrylate); SDS, sodium dodecyl sulfate; RML, rhamnolipid; PCA-HEX, *n*-hexane extract of *Piper cabralanum* C.DC.

hemolytic effect of PCA-HEX and NPs of PMMA-SDS, PMMA-RML, and PMMA-RML-PCA-HEX (Figure 7I) was investigated. The results indicate that there is no hemolytic effect at concentrations of 1,500 µg/mL (Figure 7I).

Conclusion

In this study, the characteristics of PMMA polymeric NPs with the addition of a Piperaceae plant extract were investigated. We demonstrated that extract encapsulation (PCA-HEX) was efficient and increased cytotoxic activity in K562 tumor cells. The results showed that the technique used for encapsulation has high efficiency without reducing the activity of the plant extract. For compounds with high complexity and with difficulty of encapsulation, we suggest the technique of miniemulsion and in situ polymerization for the production of core-shell NPs of PMMA. PMMA NPs are nontoxic, biocompatible, and biodegradable materials with high encapsulation capacity. PCA-HEX encapsulation increased cytotoxic activity in K562 human cells and did not induce hemolysis. Thus, core-shell NPs of PMMA may be an important alternative for the encapsulation of essential oils, extracts with phytotherapeutic activities, or antitumor compounds against leukemia and other tumor models.

Acknowledgments

The authors wish to thank Conselho Nacional de Desenvolvimento Científico e Tecnológico (CNPq), Fundação Amparo à Pesquisa do Estado do Piauí (FAPEPI), Fundação Carlos Chagas Filho de Amparo à Pesquisa do Estado do Rio de Janeiro (FAPERJ), and Coordenação de Aperfeiçoamento de Pessoal de Nível Superior (CAPES) for supporting this work and for providing scholarships.

Disclosure

The authors report no conflicts of interest in this work.

References

1. Petros RA, DeSimone JM. Strategies in the design of nanoparticles for therapeutic applications. *Nat Rev Drug Discov*. 2010;9(8):615–627.
2. Cabane E, Zhang X, Langowska K, Palivan CG, Meier W. Stimuli-responsive polymers and their applications in nanomedicine. *Biointerphases*. 2012;7(1–4):9.
3. Masood F. Polymeric nanoparticles for targeted drug delivery system for cancer therapy. *Mater Sci Eng C Mater Biol Appl*. 2016;60:569–578.
4. Thambi T, Park JH, Lee DS. Stimuli-responsive polymersomes for cancer therapy. *Biomater Sci*. 2016;4(1):55–69.
5. Rimessi P, Sabatelli P, Fabris M, et al. Cationic PMMA nanoparticles bind and deliver antisense oligoribonucleotides allowing restoration of dystrophin expression in the mdx mouse. *Mol Ther*. 2009;17(5):820–827.

6. Xie Y, Bagby TR, Cohen MS, Forrest ML. Drug delivery to the lymphatic system: importance in future cancer diagnosis and therapies. *Expert Opin Drug Deliv*. 2009;6(8):785–792.
7. Oerlemans C, Bult W, Bos M, Storm G, Nijsen JFW, Hennink WE. Polymeric micelles in anticancer therapy: targeting, imaging and triggered release. *Pharm Res*. 2010;27(12):2569–2589.
8. Shi M, Kretlow JD, Nguyen A, et al. Antibiotic-releasing porous polymethylmethacrylate constructs for osseous space maintenance and infection control. *Biomaterials*. 2010;31(14):4146–4156.
9. Adinolfi B, Pellegrino M, Giannetti A, et al. Molecular beacon-decorated polymethylmethacrylate core-shell fluorescent nanoparticles for the detection of survivin mRNA in human cancer cells. *Biosens Bioelectron*. 2017;88:15–24.
10. Sanhai WR, Sakamoto JH, Canady R, Ferrari M. Seven challenges for nanomedicine. *Nat Nanotechnol*. 2008;3(5):242–244.
11. O'Dowd-Booth CJ, White J, Smitham P, Khan W, Marsh DR. Bone cement: perioperative issues, orthopaedic applications and future developments. *J Perioper Pract*. 2011;21(9):304–308.
12. Nguyen AT, Ahmad J, Fagien S, Rohrich RJ. Cosmetic medicine: facial resurfacing and injectables. *Plast Reconstr Surg*. 2012;129(1):142e–153e.
13. Mendes AN, Hubber I, Siqueira M, et al. Preparation and cytotoxicity of poly(methyl methacrylate) nanoparticles for drug encapsulation. *Macromol Symp*. 2012;319(1):1–250.
14. Aiertza MK, Odriozola I, Cabanero G, Grande H-J, Loinaz I. Single-chain polymer nanoparticles. *Cell Mol Life Sci*. 2012;69(3):337–346.
15. Luque-Michel E, Imbuluzqueta E, Sebastian V, Blanco-Prieto MJ. Clinical advances of nanocarrier-based cancer therapy and diagnostics. *Expert Opin Drug Deliv*. 2017;14(1):75–92.
16. Dalgıç CT, Kaymaz BT, Özkan MC, Dalmızrak A, Şahin F, Saydam G. Investigating the role of JAK/STAT pthway on dasatinib-induced apoptosis for CML cell model K562. *Clin Lymphoma Myeloma Leuk*. 2015;15(Suppl):S161–S166.
17. Rumjanek VM, Vidal RS, Maia RC. Multidrug resistance in chronic myeloid leukaemia: how much can we learn from MDR–CML cell lines? *Biosci Rep*. 2013;33(6):e00081.
18. Tang R, Cohen S, Perrot J-Y, et al. P-gp activity is a critical resistance factor against AVE9633 and DM4 cytotoxicity in leukaemia cell lines, but not a major mechanism of chemoresistance in cells from acute myeloid leukaemia patients. *BMC Cancer*. 2009;9:199.
19. Faderl S, Kantarjian HM, Talpaz M. Chronic myelogenous leukemia: update on biology and treatment. *Oncology (Williston Park)*. 1999;13(2):169–180, 184.
20. Chan E-S, Yim Z-H, Phan S-H, Mansa RF, Ravindra P. Encapsulation of herbal aqueous extract through absorption with ca-alginate hydrogel beads. *Food Bioprod Process*. 2010;88(2–3):195–201.
21. Moreira DL, Fonseca VM, Bhering CA, et al. Chemical composition and antileishmanial activity from fractions of *Piper cabralanum* C.DC. (Piperaceae). *Rev Fitos*. 2013;5(1):92–98.
22. Leon-Gonzalez AJ, Acero N, Munoz-Mingarro D, Navarro I, Martin-Cordero C. Chalcones as promising lead compounds on cancer therapy. *Curr Med Chem*. 2015;22(30):3407–3425.
23. Shi Y-N, Xin Y, Ling Y, et al. Chemical constituents from *Piper hainanense* and their cytotoxicities. *J Asian Nat Prod Res*. 2016;18(8):730–736.
24. Ovadje P, Ma D, Tremblay P, et al. Evaluation of the efficacy and biochemical mechanism of cell death induction by Piper longum extract selectively in in-vitro and in-vivo models of human cancer cells. *PLoS One*. 2014;9(11):e113250.
25. Lizcano LJ, Siles M, Trepiana J, et al. *Piper* and *Vismia* species from Colombian Amazonia differentially affect cell proliferation of hepatocarcinoma cells. *Nutrients*. 2015;7(1):179–195.
26. Mendes AN, Filgueiras LA, Pinto JC, Nele M. Physicochemical properties of rhamnolipid biosurfactant from *Pseudomonas aeruginosa* PA1 to applications in microemulsions. *J Biomater Nanobiotechnol*. 2015;6:64–79.
27. Sperandio D, Rossignol G, Guerillon J, et al. Cell-associated hemolysis activity in the clinical strain of *Pseudomonas fluorescens* MFN1032. *BMC Microbiol*. 2010;10(1):124.
28. Schaffazick SR, Guterres SS, Freitas L de L, Pohlmann AR. Physicochemical characterization and stability of the polymeric nanoparticle systems for drug administration. *Quím Nov*. 2003;26:726–737.
29. Gamisans F, Lacoulonche F, Chauvet A, Espina M, Garcia ML, Egea MA. Flurbiprofen-loaded nanospheres: analysis of the matrix structure by thermal methods. *Int J Pharm*. 1999;179(1):37–48.
30. Balamurugan A, Kannan S, Selvaraj V, Rajeswari S. Development and spectral characterization of poly (methyl methacrylate)/hydroxyapatite composite for biomedical applications. *Trends Biomater Artif Organs*. 2004;18(1):41–45.
31. Pretsch E, Clerc T, Seibl J, Simon W. *Tables of Spectral Data for Structure Determination of Organic Compounds*. Berlin, Germany: Springer Science & Business Media; 2013.
32. Gao X, Zhang X, Wu Z, Zhang X, Wang Z, Li C. Synthesis and physicochemical characterization of a novel amphiphilic polylactic acid-hyperbranched polyglycerol conjugate for protein delivery. *J Control Release*. 2009;140(2):141–147.
33. Karavas E, Koutris E, Papadopoulos AG, et al. Application of density functional theory in combination with FTIR and DSC to characterise polymer drug interactions for the preparation of sustained release formulations between fluvastatin and carrageenans. *Int J Pharm*. 2014;466(1–2):211–222.
34. El-Housssiny AS, Ward AA, Mostafa DM, et al. Drug–polymer interaction between glucosamine sulfate and alginate nanoparticles: FTIR, DSC and dielectric spectroscopy studies. *Adv Nat Sci Nanosci Nanotechnol*. 2016;7(2):25014.
35. Lin S-Y, Wang S-L. Advances in simultaneous DSC–FTIR microspectroscopy for rapid solid-state chemical stability studies: some dipeptide drugs as examples. *Adv Drug Deliv Rev*. 2012;64(5):461–478.
36. Seymour RB. *Introduction to Polymer Chemistry*. Malabar, FL: RE Krieger Publishing Company; 1978.
37. Ashby MF, Cebon D. Materials selection in mechanical design. *Le J Phys IV*. 1993;3(C7):C7-1.
38. Carraher Jr CE. *Introduction to Polymer Chemistry*. Third edition. UK: CRC press; 2012.
39. Greenwood R. Review of the measurement of zeta potentials in concentrated aqueous suspensions using electroacoustics. *Adv Colloid Interface Sci*. 2003;106:55–81.
40. Lichtenstein A. Mechanism of mammalian cell lysis mediated by peptide defensins. Evidence for an initial alteration of the plasma membrane. *J Clin Invest*. 1991;88(1):93–100.
41. Barbosa CMV, Oliveira CR, Nascimento FD, et al. Biphosphinic palladacycle complex mediates lysosomal-membrane permeabilization and cell death in K562 leukaemia cells. *Eur J Pharmacol*. 2006;542(1–3):37–47.
42. Da Silva-Souza HA, Lira MN De, Costa-Junior HM, et al. Inhibitors of the 5-lipoxygenase arachidonic acid pathway induce ATP release and ATP-dependent organic cation transport in macrophages. *Biochim Biophys Acta – Biomembr*. 2014;1838(7):1967–1977.
43. Tramontina F, Karl J, Gottfried C, et al. Digitonin-permeabilization of astrocytes in culture monitored by trypan blue exclusion and loss of S100B by ELISA. *Brain Res Protoc*. 2000;6(1–2):86–90.